

An Acyl-NHC Osmium Cooperative System: Coordination of Small Molecules and Heterolytic B–H and O–H Bond Activation

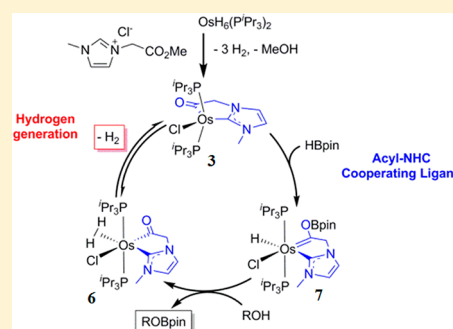
Tamara Bolaño,[†] Miguel A. Esteruelas,^{*,†} M. Pilar Gay,[†] Enrique Oñate,[†] Isidro M. Pastor,[‡] and Miguel Yus^{*,‡}

[†]Departamento de Química Inorgánica, Instituto de Síntesis Química y Catálisis Homogénea (ISQCH), Centro de Innovación en Química Avanzada (ORFEO-CINQA), Universidad de Zaragoza-CSIC, 50009 Zaragoza, Spain

[‡]Departamento de Química Orgánica, Facultad de Ciencias-Instituto de Síntesis Orgánica (ISO), Centro de Innovación en Química Avanzada (ORFEO-CINQA), Universidad de Alicante, Apdo. 99, 03080 Alicante, Spain

S Supporting Information

ABSTRACT: The hexahydride complex $\text{OsH}_6(\text{P}^i\text{Pr}_3)_2$ (**1**) activates the C–OMe bond of 1-(2-methoxy-2-oxoethyl)-3-methylimidazolium chloride (**2**), in addition to promoting the direct metalation of the imidazolium group, to afford a five-coordinate $\text{OsCl}(\text{acyl-NHC})(\text{P}^i\text{Pr}_3)_2$ (**3**) compound. The latter coordinates carbon monoxide, oxygen, and molecular hydrogen to give the corresponding carbonyl (**4**), dioxygen (**5**), and dihydrogen (**6**) derivatives. Complex **3** also promotes the heterolytic bond activation of pinacolborane (HBpin), using the acyl oxygen atom as a pendant Lewis base. The hydride ligand and the Bpin substituent of the Fischer-type carbene of the resulting complex **7** activate the O–H bond of alcohols and water. As a consequence, complex **3** is a metal ligand cooperating catalyst for the generation of molecular hydrogen, by means of both the alcoholysis and hydrolysis of pinacolborane, via the intermediates **7** and **6**.



INTRODUCTION

Catalysts based on cooperative ligands are a promising alternative for reactions associated with conversion and storage of regenerative energy.¹ These ligands cooperate with the metal center by participating directly in a σ -bond activation stage and, subsequently, by performing the reversible structural change in the process of product formation.² The outer-sphere catalysis takes place with no formal change in the metal oxidation state. The heterolytic σ -bond activation is promoted by a coordinated (Noyori–Morris type)³ or free (Shvo type)⁴ Lewis base at the cooperating ligand or by means of the aromatization of the central ring of a pincer ligand (Milstein type).⁵

The ability of the N-heterocyclic carbene (NHC) ligands to modify the electron density of the metallic core⁶ has made the NHC transition-metal complexes powerful tools in homogeneous catalysis. These ligands are easily accessible from imidazoles, which can be functionalized on both nitrogen atoms. As a consequence, a variety of excellent promoters for enantioselective processes have been developed.⁷ Because the vast majority of the NHC ligands are substituted at nitrogen by alkyl and/or aryl groups, examples of nonchiral catalysts based on NHC ligands containing an additional Lewis base are rare.⁸ The scarce catalysts known of this type are centered on hemilabile systems and have been used in functionalization reactions.⁹ In addition, some examples of complexes bearing protic NHC ligands acting as bifunctional systems have been also reported.¹⁰ An added problem for the use of NHC ligands in metal–ligand cooperating catalysis is to keep the cooperation capacity between the Lewis base tethered to the imidazole

moiety and the metal center, after the carbene coordination. In this context, access to NHC transition-metal complexes able to promote the heterolytic activation of σ bonds is challenging.

We now show a synthetic strategy that allows keeping the cooperative capacity between the additional Lewis base, tethered to the imidazole moiety, and the metal center after the carbene coordination.

RESULTS AND DISCUSSION

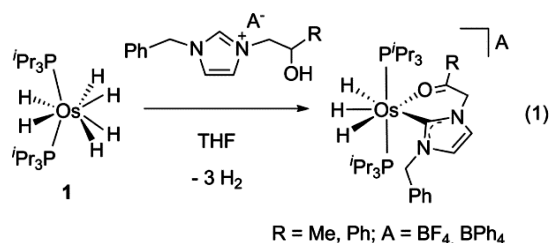
Formation of a Chelated Functional NHC-Acyl Ligand.

The complex $\text{OsH}_6(\text{P}^i\text{Pr}_3)_2$ (**1**) has been proven to promote the direct metalation of imidazolium and benzimidazolium salts,¹¹ due to its capacity for activating σ bonds.¹² The reactions have afforded a wide range of NHC complexes, with interesting properties. With alcohol-functionalized imidazolium salts, hemilabile-chelate NHC-keto compounds are formed as a result of the direct metalation of the imidazolium unit and the dehydrogenation of the alcohol function (eq 1).¹³

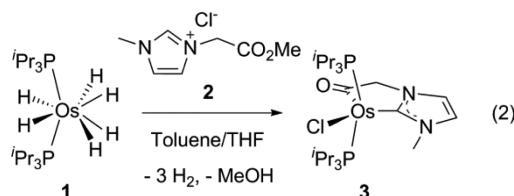
Imidazolium cations containing a carboxylic ester function have been prepared by quaternization of 1-methylimidazole with chlorocarboxylic acid ester. Methyl chloroacetate affords 1-(2-methoxy-2-oxoethyl)-3-methylimidazolium chloride (**2**).¹⁴ In comparison with the alcohol function, the ester group has the advantage of the presence of a potential sacrificial –OR group. The cleavage of the OC–OR bond should allow an acyl coordination, which would protect the carbonyl oxygen atom.

Received: June 9, 2015

Published: July 29, 2015



Furthermore, the ester prevents undesirable secondary reactions typical of aldehydes.¹⁵ In the search for osmium NHC cooperating systems, we performed the reaction of **1** with **2**, which led to **3** (eq 2) as a result of the direct metalation of



the imidazolium moiety, the cleavage of the C–OMe bond of **2** to afford methanol (detected by GC-MS), the release of three hydrogen molecules, and the coordination of the anion of the starting salt to the metal center.

Figure 1 shows the structure of **3**. The geometry around the osmium atom can be described as a distorted trigonal

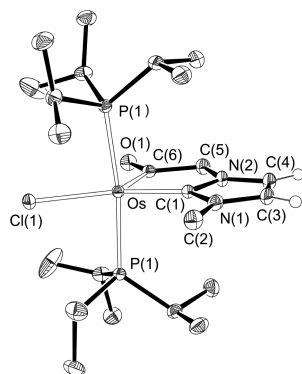


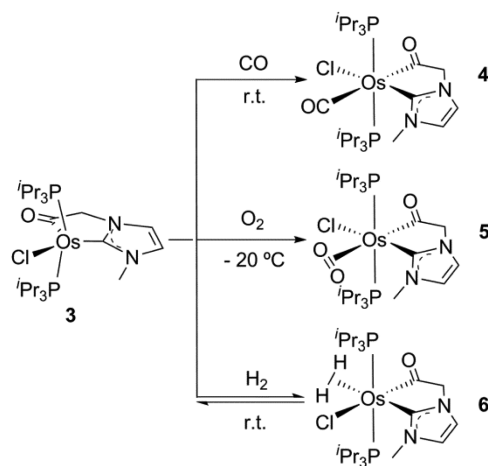
Figure 1. Molecular diagram of complex **3** (50% probability ellipsoids). Most of the hydrogen atoms are omitted for clarity. Selected bond lengths (Å) and angles (deg): Os–C(1) = 1.970(3), Os–C(6) = 1.956(3), Os–Cl(1) = 2.4552(8), Os–P(1) = 2.4130(6), O(1)–C(6) = 1.235(4), C(5)–C(6) = 1.549(4), C(3)–C(4) = 1.339(5), N(1)–C(1) = 1.359(4), N(1)–C(2) = 1.457(4), N(2)–C(5) = 1.433(4), N(2)–C(1) = 1.372(4); C(6)–Os–C(1) = 78.41(13), C(1)–Os–Cl(1) = 157.60(10), C(6)–Os–Cl(1) = 123.99(10), P(1)–Os–P(1) = 172.37(3).

bipyramid with apical phosphines and inequivalent angles within the Y-shaped equatorial plane (C(1)–Os–C(6) = 78.41(3)°, Cl(1)–Os–C(1) = 157.60(10)°, and Cl(1)–Os–C(6) = 123.99(10)°). The Os–C(6) and C(6)–O(1) bond lengths of 1.956(3) and 1.235(4) Å, respectively, support the osmium acyl formulation,¹⁶ whereas the Os–C(1) distance of 1.970(3) Å is consistent with a normal coordination of the NHC unit.^{11,13} In agreement with the presence of the acyl group, the IR contains a characteristic $\nu(\text{CO})$ band at 1623 cm^{−1}. In the ¹³C{¹H} NMR spectrum, the acyl resonance appears at 217.9 ppm as a singlet, whereas the metalated

carbene carbon atom displays a triplet ($J_{\text{C-P}} = 6.8$ Hz) at 173.3 ppm.

Coordination of Small Molecules. The coordination number 6 for **3** can be achieved by coordination of small molecules such as carbon monoxide, dioxygen, and dihydrogen. The reactions lead to octahedral *trans*-phosphine derivatives (Scheme 1).

Scheme 1



Stirring toluene solutions of **3** under an atmosphere of carbon monoxide affords the monocarbonyl derivative **4**. Figure 2 shows a view of its structure. The carbonyl group lies in the

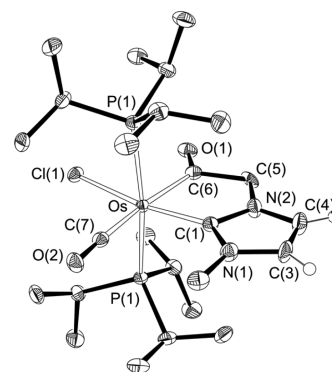


Figure 2. Molecular diagram of complex **4** (50% probability ellipsoids). Most of the hydrogen atoms are omitted for clarity. Selected bond lengths (Å) and angles (deg): Os–C(1) = 2.019(4), Os–C(7) = 1.882(4), Os–C(6) = 2.124(4), Os–Cl(1) = 2.4973(10), Os–P(1) = 2.4264(7), O(1)–C(6) = 1.218(5), O(2)–C(7) = 1.171(5), C(5)–C(6) = 1.574(6), C(3)–C(4) = 1.341(6), N(1)–C(1) = 1.372(5), N(1)–C(2) = 1.441(5), N(2)–C(5) = 1.430(5), N(2)–C(1) = 1.367(5); C(6)–Os–C(1) = 78.91(16), C(7)–Os–Cl(1) = 94.53(16), C(7)–Os–Cl(1) = 98.72(12), C(1)–Os–Cl(1) = 166.75(11), C(6)–Os–Cl(1) = 87.84(11), P(1)–Os–P(1) = 170.01(4).

plane perpendicular to the P–Os–P direction, avoiding competition by the electron density of the metal center with the also π -acidic imidazolidene moiety.^{11d} Thus, it is *trans*-disposed to the acyl unit (C(6)–Os–C(7) = 173.44(17)°). The carbonyl coordination produces a certain weakening of the Os–C(acyl) bond, suggesting that, in addition to the acyl to osmium σ donation, there is also some back-bonding. As a result, the Os–C(6) distance (2.124(4) Å) lengthens by about

0.17 Å with regard to that in **3**. In addition, the acyl resonance (δ , 267.6 ppm) in the $^{13}\text{C}\{^1\text{H}\}$ NMR spectrum undergoes a shift of about 50 ppm toward lower field.

Complex **3** gives the dioxygen compound **5** under an atmosphere of oxygen in toluene, at -20°C . A drawing of its structure is shown in Figure 3. In agreement with a noticeable

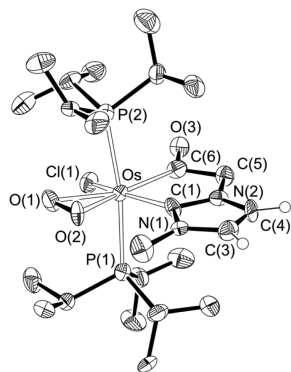


Figure 3. Molecular diagram of complex **5** (50% probability ellipsoids). Most of the hydrogen atoms are omitted for clarity. Selected bond lengths (Å) and angles (deg): Os–C(1) = 2.065(11), Os–C(6) = 2.066(11), Os–Cl(1) = 2.414(3), Os–O(1) = 2.079(8), Os–O(2) = 2.072(7), Os–P(1) = 2.456(3), Os–P(2) = 2.445(3), O(1)–O(2) = 1.396(10), O(3)–C(6) = 1.207(12), C(5)–C(6) = 1.582(16), C(3)–C(4) = 1.365(15), N(1)–C(1) = 1.375(13), N(1)–C(2) = 1.477(13), N(2)–C(5) = 1.457(13), N(2)–C(1) = 1.385(14); C(1)–Os–C(6) = 78.1(5), C(1)–Os–O(2) = 82.2(3), C(6)–Os–O(2) = 158.5(4), C(1)–Os–O(1) = 121.5(4), C(6)–Os–O(1) = 158.8(4), O(2)–Os–O(1) = 39.3(3), O(2)–Os–Cl(1) = 119.9(2), O(1)–Os–Cl(1) = 81.2(2), C(6)–Os–Cl(1) = 81.1(4), P(2)–Os–P(1) = 171.63(12).

π -acceptor character, the coordinated oxygen molecule is trans-disposed to the acyl group at the plane perpendicular to the P–Os–P direction, as the carbonyl ligand of **4**. The oxygen atoms are symmetrically bound to osmium with identical Os–O bond lengths of 2.072(7) and 2.079(8) Å within standard deviations. The O–O distance of 1.396(10) Å is in the middle of the range observed for $\text{Os}(\eta^2\text{-O}_2)$ derivatives (1.31–1.49 Å)¹⁷ and, along with the $\nu(\text{O}=\text{O})$ stretching band at 962 cm^{-1} , supports the peroxide formulation.¹⁸ The coordination of the oxygen molecule also weakens the Os–C(acyl) bond, although the effect is less pronounced than in the carbonyl case. Thus, the Os–C(6) bond length of 2.066(11) Å is about 0.11 Å longer than in **3** but about 0.06 Å shorter than in **4**. Most of the $\text{Os}(\eta^2\text{-O}_2)$ derivatives are of the type $[\text{OsX}(\eta^2\text{-O}_2)(\text{P-P})]^+$ (X = H, Cl; P–P = diphosphine), which increase their stability by increasing the basicity of the ligands.¹⁷ Some stable adducts have been also formed in the presence of π -acidic groups such as $\text{OsHCl}(\eta^2\text{-O}_2)(\text{PR}_3)_2$ ($\text{PR}_3 = \text{PCy}_3$,¹⁹ P^iPr_3 ²⁰). Complex **5** is the first member of a new family of $\text{Os}(\eta^2\text{-O}_2)$ compounds. Unfortunately, its stability is much lower; at temperatures higher than -20°C , **5** irreversibly loses $\text{O}=\text{P}^i\text{Pr}_3$.

Complex **3** adds molecular hydrogen to afford the dihydrogen compound **6**, under a hydrogen atmosphere, in toluene at room temperature. In contrast to carbon monoxide and oxygen, the coordination of the hydrogen molecule is reversible. The replacement of the hydrogen atmosphere by argon regenerates **3**. This difference in behavior is a consequence of the scarce π -acceptor power of the hydrogen ligand and its low σ -donation capacity. Figure 4 shows a drawing of the molecule of **6**. In contrast to carbon monoxide

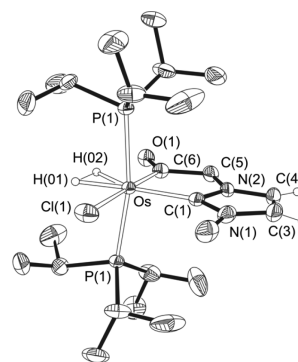
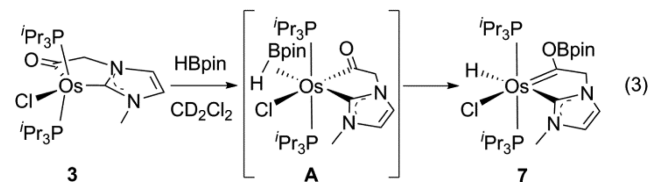


Figure 4. Molecular diagram of complex **6** (50% probability ellipsoids). Most of the hydrogen atoms are omitted for clarity. Selected bond lengths (Å) and angles (deg): Os–C(1) = 2.065(6), Os–C(6) = 1.998(9), Os–Cl(1) = 2.547(3), Os–P(1) = 2.4019(10), Os–H(01) = 1.596(12), Os–H(02) = 1.592(12), C(5)–C(6) = 1.539(11), C(3)–C(4) = 1.329(5), N(2)–C(1) = 1.371(7), N(2)–C(4) = 1.384(5), N(1)–C(2) = 1.528(13), N(1)–C(1) = 1.385(8); C(6)–Os–C(1) = 79.5(3), C(1)–Os–Cl(1) = 98.26(11), C(6)–Os–Cl(1) = 177.7(3), P(1)–Os–P(1) = 168.83(5).

and oxygen, the hydrogen molecule coordinates trans to the π -acceptor imidazolidene moiety. The hydrogen atoms—separated by 1.1 (1) Å—are located in the plane perpendicular to the P–Os–P direction. Retainment of the H–H bond after the dihydrogen coordination is also supported by the ^1H NMR spectrum, in toluene- d_8 , which contains the characteristic dihydrogen resonance at -4.50 ppm with a 300 MHz $T_1(\text{min})$ value of 8 ± 1 ms at 223 K. This value corresponds to a H–H distance of 0.80 Å (fast spinning) or 1.0 Å (slow spinning).²¹ In accordance with the latter, a H–D coupling constant of 23.1 Hz was obtained from the species containing the partially deuterated $\eta^2\text{-HD}$ ligand.²²

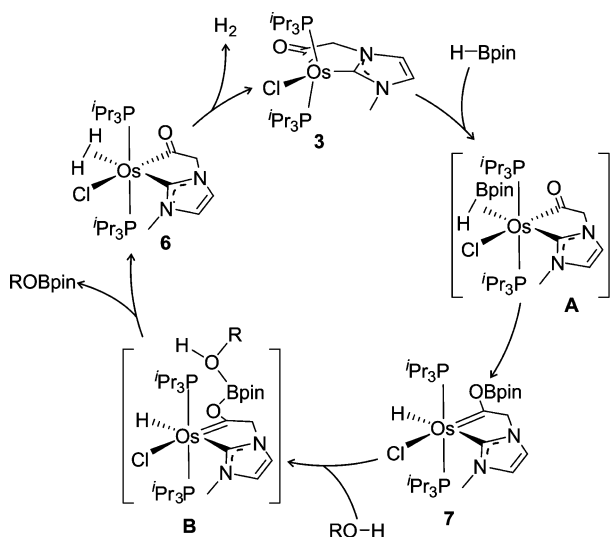
Alcoholysis and Hydrolysis of Pinacolborane. The comparison of the structures shown in Figures 2–4 suggests that the coordination of σ bonds to **3** is favored at the positions trans to the imidazolidene moiety. Due to the π -acceptor character of this unit,^{10d} the interaction should mainly involve σ donation from the σ orbital of the coordinated bond to empty orbitals of the metal. The ligand to metal nature of the donation would favor the heterolytic cleavage of the σ bond, which could use the oxygen atom of the *cis*-acyl group as a pendant Lewis base. In fact, in contrast to molecular hydrogen, the polar B–H bond of pinacolborane (HBpin) undergoes heterolytic bond activation.²³ The addition of 1.0 equiv of the boron hydride to dichloromethane- d_2 solutions of **3**, contained in an NMR tube, affords **7**, in an instantaneous and quantitative manner (eq 3). Its formation, which does not imply any change



is the formal metal oxidation state, is mainly supported by the ^1H and $^{11}\text{B}\{^1\text{H}\}$ NMR spectra of the resulting solution. The former contains a triplet ($J_{\text{H-P}} = 26.4$ Hz) at -9.32 ppm with an integrated intensity of 1 corresponding to the hydride ligand, whereas the latter shows a characteristic $\text{B}(\text{OR})_3$ resonance at 19.2 ppm.

The hydride ligand and the Bpin substituent of the generated Fischer-type carbene activate the O–H bond of alcohols and water, via an outer-sphere process, in a heterolytic manner. As a result, complex **7** is extremely sensitive to the dampness of the solvent and even to the presence of –OH groups in the glassware. These reactions and those with alcohols give ROBpin and the dihydrogen derivative **6**, which loses the coordinated hydrogen molecule to regenerate **3**. The formation of **7** according to eq 3, the outer-sphere activation of RO–H bonds, and the release of H₂ to regenerate **3** constitute a stoichiometric cycle for the generation of molecular hydrogen by means of the alcoholysis of HBpin (Scheme 2).

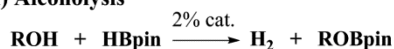
Scheme 2



According to this cycle, complex **3** catalyzes the kinetically controlled alcoholysis of pinacolborane, as well as its hydrolysis (Scheme 3). These reactions were performed in toluene at 30

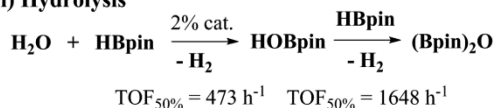
Scheme 3

i) Alcoholysis



R (TOF_{50%}, h^{−1}) = methyl (3644), ethyl (2108), *n*-butyl (1395), *n*-octyl (1364), benzyl (1393), isopropyl (365), *t*-butyl (62), phenyl (313)

ii) Hydrolysis



°C using 2 mol % of catalyst and HBpin and ROH concentrations of 0.276 M. The amount of H₂ generated was measured by displacing Vaseline oil from a gas buret.

Primary, secondary, and tertiary alcohols, as well as phenol, were successfully used to generate molecular hydrogen and ROBpin in a quantitative manner, with turnover frequencies at 50% conversion (TOF_{50%}) between 3644 and 62 h^{−1} (Scheme 3i). The bulkiness of the alcohol determines its efficiency, which decreases in the sequence primary > secondary > tertiary. In a consistent manner, for primary alcohols, the reaction rates decrease as the length of the carbon chain increases: i.e., methanol > ethanol > 1-butanol > 1-octanol. Benzyl alcohol

generates H₂ with a TOF_{50%} value similar to that of 1-butanol. 2-Propanol presents a TOF_{50%} value similar to that of 1-butanol and is about 10 times less efficient than methanol, whereas *tert*-butyl alcohol is about 6 times less efficient than 2-propanol. The reaction rate with phenol is similar to that with 2-propanol.

The hydrolysis (Scheme 3ii) is sequential. By using a H₂O/HBpin molar ratio of 1/1, HOBpin is exclusively formed with a TOF_{50%} value of 473 h^{−1}. Subsequently, HOBpin reacts with a second equivalent of HBpin to afford (Bpin)₂O with a TOF_{50%} value of 1648 h^{−1}, which is about 3.5 times faster than the first reaction. The low TOF_{50%} value observed for the formation of HOBpin appears to be a consequence of the low solubility of H₂O in toluene, whereas the high selectivity in its formation, along with the influence of the alcohol size in the alcoholysis, suggests that the outer-sphere RO–H bond activation is a two-stage process (Scheme 2). Initially, the coordination of the oxygen atom of ROH to the acidic boron atom of **7**, to afford **B**, takes place. In the second step, the transfer of the OH proton to the hydride and the concerted release of ROBpin from **B** occur, to form **6**. Thus, the catalysis rate is a function of the formation constant of **B** and the rate constant of the proton transfer. The former value increases as the bulkiness of the R substituent decreases, while the latter value increases as the bulkiness of the R substituent increases.

■ CONCLUDING REMARKS

In conclusion, the reactions of hydride complexes with imidazolium cations with a tethered carboxylic ester function at one of the nitrogen atoms allow the preparation of complexes containing a chelated functional NHC-acyl ligand, as a result of the direct metalation of the imidazolium moiety and the C–OR bond activation on the ester function. Through this novel strategy, in this paper, we show the synthesis of the five-coordinate complex **3**. This compound is a metal ligand cooperating catalyst for the generation of molecular hydrogen by means of both the alcoholysis and the hydrolysis of pinacolborane. This property is a direct consequence of the capacity of **3** for coordinating small molecules, including σ bonds, and for promoting the heterolytic B–H bond activation of boranes using the acyl oxygen atom as a pendant Lewis base.

■ EXPERIMENTAL SECTION

All reactions were carried out with rigorous exclusion of air using Schlenk-tube techniques or in an argon-filled Unilab glovebox (O₂ levels below 0.6 ppm). Glassware was previously pretreated with 5% Me₃SiCl in dichloromethane solution, to silylate the glass surface. Acetone, methanol, tetrahydrofuran, and 2-propanol were dried and distilled under argon. Other solvents were obtained oxygen- and water-free from an MBraun solvent purification apparatus; additionally, pentane was treated with P₂O₅. Alcohols were dried by standard procedures and distilled under argon prior to use. Pinacolborane (HBpin; 4,4,5,5-tetramethyl-1,3,2-dioxaborolane) and all other reagents were purchased from commercial sources and used without further purification. NMR spectra were recorded on a Varian Gemini 2000, a Bruker ARX 300 MHz, a Bruker Avance 300 MHz, or a Bruker Avance 400 MHz instrument. Chemical shifts (expressed in parts per million) are referenced to residual solvent peaks (¹H, ¹H{³¹P}, ¹³C{¹H}) or external standard (³¹P{¹H} to 85% H₃PO₄ and ¹¹B to BF₃·OEt₂). Coupling constants *J* and *N* (*N* = *J*(PH) + *J*(P'H) for ¹H and *N* = *J*(PC) + *J*(P'C) for ¹³C{¹H}) are given in hertz. Attenuated total reflection infrared spectra (ATR-IR) of solid samples were run on a PerkinElmer Spectrum 100 FT-IR spectrometer. C, H, and N analyses were carried out in a PerkinElmer 2400 CHNS/O analyzer. High-resolution electrospray mass spectra (HRMS) were acquired using a MicroTOF-Q hybrid quadrupole time-of-flight spectrometer

(Bruker Daltonics, Bremen, Germany). $\text{OsH}_6(\text{P}^i\text{Pr}_3)_2$ and 1-(2-methoxy-2-oxoethyl)-3-methylimidazolium chloride were prepared according to the published methods.^{13,24}

Preparation of $\text{OsCl}[\kappa^2\text{-C,C-}[\text{CN}(\text{CH}_3)\text{CHCHNCH}_2\text{C}(\text{O})]](\text{P}^i\text{Pr}_3)_2$ (3). $\text{OsH}_6(\text{P}^i\text{Pr}_3)_2$ (0.500 g, 0.968 mmol) was dissolved in a 1/1 THF/toluene mixture (10 mL) and treated with 1-(2-methoxy-2-oxoethyl)-3-methylimidazolium chloride (0.220 g, 1.154 mmol). The mixture was stirred under reflux for 3 h before the volatiles were removed under vacuum. Subsequent addition of methanol (2 mL) to the resulting residue, at approximately -70°C , led to the formation of a reddish brown solid, which was washed with further portions of diethyl ether (2×3 mL) and dried in vacuo. Yield: 0.480 g (74%). Orange crystals suitable for X-ray diffraction analysis were obtained from a concentrated solution of **1** in acetone. Anal. Calcd for $\text{C}_{24}\text{H}_{49}\text{ClN}_2\text{O}_2\text{OsP}_2$: C, 43.07; H, 7.38; N, 4.19. Found: C, 42.69; H, 7.77; N, 4.16. HRMS (electrospray, m/z): calcd for $\text{C}_{24}\text{H}_{49}\text{N}_2\text{O}_2\text{OsP}_2$ $[\text{M} - \text{Cl}]^+$ 635.2930, found 635.2963. IR (cm^{-1}): $\nu(\text{C}=\text{O})$ 1623 (s). ^1H NMR (400 MHz, $(\text{CD}_3)_2\text{CO}$, 293 K): δ 7.33 and 6.95 (both d, $J_{\text{H-H}} = 2.0$, 1 H each, $\text{CH}_{\text{imidazole}}$), 3.96 (s, 3 H, NCH_3), 2.77 (s, 2 H, NCH_2), 2.58 (m, 6 H, PCH), 1.16 (dvt, $N = 13.2$, $J_{\text{H-H}} = 7.2$, 18 H, $\text{PCH}(\text{CH}_3)_3$), 1.09 (dvt, $N = 12.4$, $J_{\text{H-H}} = 6.8$, 18 H, $\text{PCH}(\text{CH}_3)_3$). $^{31}\text{P}\{^1\text{H}\}$ NMR (162 MHz, $(\text{CD}_3)_2\text{CO}$, 293 K): δ 23.3 (s). $^{13}\text{C}\{^1\text{H}\}$ -APT NMR plus HMBC and HSQC (75.5 MHz, C_6D_6 , 293 K): δ 217.9 (s, $\text{C}=\text{O}$), 173.3 (t, $J_{\text{C-P}} = 6.8$, NCN), 120.1 and 114.1 (both s, $\text{CH}_{\text{imidazole}}$), 69.9 (s, NCH_2), 38.0 (s, NCH_3), 24.4 (vt, $N = 22.7$, PCH), 21.0 and 19.7 (both s, $\text{PCH}(\text{CH}_3)_3$).

Reaction of 3 with CO: Formation of $\text{OsCl}[\kappa^2\text{-C,C-}[\text{CN}(\text{CH}_3)\text{CHCHNCH}_2\text{C}(\text{O})]](\text{CO})(\text{P}^i\text{Pr}_3)_2$ (4). A solution of **3** (0.088 g, 0.131 mmol) in toluene (5 mL) was stirred under a CO atmosphere (1 atm) at room temperature for 5 min. The resulting colorless solution was reduced to dryness. Addition of diethyl ether (3 mL) to the residue obtained led to the formation of a white solid, which was washed with additional portions of diethyl ether (2×3 mL) and dried in vacuo. Yield: 0.037 g (40%). Colorless crystals suitable for X-ray diffraction analysis were obtained from a concentrated solution of **4** in acetone. Anal. Calcd for $\text{C}_{25}\text{H}_{49}\text{ClN}_2\text{O}_2\text{OsP}_2$: C, 43.06; H, 7.08; N, 4.02. Found: C, 42.66; H, 7.41; N, 4.31. HRMS (electrospray, m/z): calcd for $\text{C}_{25}\text{H}_{49}\text{N}_2\text{O}_2\text{OsP}_2$ $[\text{M} - \text{Cl}]^+$ 663.2879, found 663.2925. IR (cm^{-1}): $\nu(\text{C}=\text{O})$ 1910 (s), $\nu(\text{C}=\text{O})$ 1597 (m). ^1H NMR (300 MHz, CD_2Cl_2 , 293 K): δ 7.05 and 6.74 (both d, $J_{\text{H-H}} = 2.1$, 1 H each, $\text{CH}_{\text{imidazole}}$), 3.93 (s, 3 H, NCH_3), 3.59 (s, 2 H, NCH_2), 2.48 (m, 6 H, PCH), 1.25 (dvt, $N = 13.6$, $J_{\text{H-H}} = 7.0$, 18 H, $\text{PCH}(\text{CH}_3)_3$), 0.95 (dvt, $N = 12.9$, $J_{\text{H-H}} = 6.6$, 18 H, $\text{PCH}(\text{CH}_3)_3$). $^{31}\text{P}\{^1\text{H}\}$ NMR (121.5 MHz, CD_2Cl_2 , 293 K): δ 1.1 (s). $^{13}\text{C}\{^1\text{H}\}$ -APT NMR plus HSQC and HMBC (75.5 MHz, CD_2Cl_2 , 293 K): δ 267.6 (t, $J_{\text{C-P}} = 11.0$, $\text{C}=\text{O}$), 194.8 (t, $J_{\text{C-P}} = 9.4$, $\text{C}=\text{O}$), 167.9 (s, NCN), 123.2 and 117.9 (both s, $\text{CH}_{\text{imidazole}}$), 71.7 (s, NCH_2), 39.1 (s, NCH_3), 25.6 (vt, $N = 24.9$, PCH), 20.7 and 19.2 (both s, $\text{PCH}(\text{CH}_3)_3$).

Reaction of 3 with O_2 : Formation of $\text{OsCl}[\kappa^2\text{-C,C-}[\text{CN}(\text{CH}_3)\text{CHCHNCH}_2\text{C}(\text{O})]](\eta^2\text{-O}_2)(\text{P}^i\text{Pr}_3)_2$ (5). A solution of **3** (0.100 g, 0.149 mmol) in toluene (5 mL) was stirred under an O_2 atmosphere (1 atm) at -20°C for 15 min. After removal of volatiles, diethyl ether (3×3 mL) was added to extract the product. The diethyl solution was concentrated to ca. 4 mL and placed in the freezer (-30°C). Red crystals corresponding to **5**, suitable for X-ray diffraction analysis, were grown. IR (cm^{-1}): $\nu(\text{C}=\text{O})$ 1621 (s), $\nu(\text{O}-\text{O})$ 962 (s). ^1H NMR (300 MHz, CD_2Cl_2 , 253 K): δ 7.16 and 6.97 (both d, $J_{\text{H-H}} = 2.1$, 1 H each, $\text{CH}_{\text{imidazole}}$), 4.23 (s, 3 H, NCH_3), 3.90 (s, 2 H, NCH_2), 2.37 (m, 6 H, PCH), 1.09 (dvt, $N = 13.1$, $J_{\text{H-H}} = 6.8$, 18 H, $\text{PCH}(\text{CH}_3)_3$), 1.08 (dvt, $N = 13.1$, $J_{\text{H-H}} = 6.2$, 18 H, $\text{PCH}(\text{CH}_3)_3$). $^{31}\text{P}\{^1\text{H}\}$ NMR (121.5 MHz, CD_2Cl_2 , 253 K): δ -23.6 (s). $^{13}\text{C}\{^1\text{H}\}$ NMR plus HSQC and HMBC (75.5 MHz, CD_2Cl_2 , 233 K): δ 250.8 (br, $\text{C}=\text{O}$), 156.2 (s, NCN), 127.3 and 118.9 (both s, $\text{CH}_{\text{imidazole}}$), 76.1 (s, NCH_2), 38.4 (s, NCH_3), 22.3 (br, PCH), 18.1 and 16.5 (both s, $\text{PCH}(\text{CH}_3)_3$).

Reaction of 3 with H_2 : Formation of $\text{OsCl}[\kappa^2\text{-C,C-}[\text{CN}(\text{CH}_3)\text{CHCHNCH}_2\text{C}(\text{O})]](\eta^2\text{-H}_2)(\text{P}^i\text{Pr}_3)_2$ (6). A J. Young NMR tube was charged with a solution of **3** (0.010 g, 0.015 mmol) in C_6D_6 (0.5 mL). Argon was replaced by H_2 (1 atm), causing the red solution to turn pale yellow. The immediate and quantitative evolution of **3** to **6** was observed by ^1H , $^{31}\text{P}\{^1\text{H}\}$, and $^{13}\text{C}\{^1\text{H}\}$ NMR spectroscopy. ^1H NMR

(300 MHz, C_6D_6 , 293 K): δ 6.21 and 5.99 (both d, $J_{\text{H-H}} = 1.7$, 1 H each, $\text{CH}_{\text{imidazole}}$), 4.24 (s, 3 H, NCH_3), 3.12 (s, 2 H, NCH_2), 2.49 (m, 6 H, PCH), 1.20 (dvt, $N = 12.8$, $J_{\text{H-H}} = 6.8$, 18 H, $\text{PCH}(\text{CH}_3)_3$), 1.01 (dvt, $N = 12.9$, $J_{\text{H-H}} = 6.9$, 18 H, $\text{PCH}(\text{CH}_3)_3$), -4.63 (t, $J_{\text{H-P}} = 8.7$, 2 H, OsH). $^{31}\text{P}\{^1\text{H}\}$ NMR (121.5 MHz, C_6D_6 , 293 K): δ 12.5 (s). $^{13}\text{C}\{^1\text{H}\}$ -APT NMR plus HSQC and HMBC (75.5 MHz, C_6D_6 , 293 K): δ 233.8 (t, $J_{\text{C-P}} = 6.0$, $\text{C}=\text{O}$), 180.6 (t, $J_{\text{C-P}} = 7.6$, NCN), 124.0 and 116.7 (both s, $\text{CH}_{\text{imidazole}}$), 72.8 (s, NCH_2), 37.7 (s, NCH_3), 24.9 (vt, $N = 24.2$, PCH), 19.3 and 19.2 (both s, $\text{PCH}(\text{CH}_3)_3$). $T_{1(\text{min})}$ (ms, OsH, 300 MHz, toluene- d_8 , 223 K): 8 ± 1 (-4.50 ppm).

Determination of the $J_{\text{H-D}}$ Value for Complex 6 (6'). A J. Young NMR tube was charged with a solution of **3** (0.010 g, 0.015 mmol) in toluene- d_8 (0.5 mL). Argon was replaced by HD (1 atm), which was generated in situ by reaction of NaH with D_2O . An immediate color change from red to pale yellow was observed in the solution. The ^1H and $^1\text{H}\{^{31}\text{P}\}$ NMR spectra, in a 300 MHz apparatus at 293 K, of this solution exhibit a triplet with $J_{\text{H-D}} = 23.1$ Hz in the hydride region.

Reaction of 3 with Pinacolborane: Formation of $\text{OsHCl}[\kappa^2\text{-C,C-}[\text{CN}(\text{CH}_3)\text{CHCHNCH}_2\text{C}(\text{OBPin})]](\text{P}^i\text{Pr}_3)_2$ (7). In a NMR tube, a reddish brown suspension of **3** (0.028 g, 0.042 mmol) in CD_2Cl_2 (0.5 mL) was treated at room temperature with pinacolborane (0.007 μL , 0.046 mmol). Immediately the initial suspension disappeared and an intense pink solution was observed. The quantitative formation of a new species corresponding to **7** was confirmed by ^1H , $^{31}\text{P}\{^1\text{H}\}$, ^{11}B , and $^{13}\text{C}\{^1\text{H}\}$ NMR spectroscopy. ^1H NMR (300 MHz, CD_2Cl_2 , 293 K): δ 7.08 and 6.79 (both d, $J_{\text{H-H}} = 2.0$, 1 H each, $\text{CH}_{\text{imidazole}}$), 4.33 (s, 3 H, NCH_3), 2.33 (m, 6 H, PCH), 1.56 (t, $J_{\text{H-P}} = 3.3$, 2 H, NCH_2), 1.28 (dvt, $N = 12.6$, $J_{\text{H-H}} = 6.9$, 18 H, $\text{PCH}(\text{CH}_3)_3$), 1.24 (s, 12 H, $\text{CH}_3\text{-BPin}$), 0.93 (dvt, $N = 13.2$, $J_{\text{H-H}} = 7.2$, 18 H, $\text{PCH}(\text{CH}_3)_3$), -9.32 (t, $J_{\text{H-P}} = 26.4$, 1 H, OsH). $^{31}\text{P}\{^1\text{H}\}$ NMR (121.5 MHz, CD_2Cl_2 , 293 K): δ 26.9 (s). ^{11}B NMR (96.3 MHz, CD_2Cl_2 , 293 K): δ 19.2 (br). $^{13}\text{C}\{^1\text{H}\}$ -APT NMR plus HSQC and HMBC (75.5 MHz, C_6D_6 , 293 K): δ 233.7 (t, $J_{\text{C-P}} = 11.3$, $\text{Os}=\text{C}(\text{OBPin})$), 185.6 (t, $J_{\text{C-P}} = 1.5$, NCN), 123.3 and 116.0 (both s, $\text{CH}_{\text{imidazole}}$), 83.6 (s, C-Bpin), 77.0 (s, NCH_2), 37.1 (s, NCH_3), 26.1 (vt, $N = 24.2$, PCH), 25.0 (s, $\text{CH}_3\text{-BPin}$), 19.6 and 19.2 (both s, $\text{PCH}(\text{CH}_3)_3$).

Alcoholysis Reactions of Pinacolborane Catalyzed by $\text{OsCl}[\kappa^2\text{-C,C-}[\text{CN}(\text{CH}_3)\text{CHCHNCH}_2\text{C}(\text{O})]](\text{P}^i\text{Pr}_3)_2$ (3). In a typical procedure, the alcohol (except for PhOH, which was dissolved in 400 μL of toluene) (1.38 mmol) was added via syringe to a solution of the catalyst (2.8×10^{-2} mmol) and HBPin (1.38 mmol) in toluene (5 mL) placed in a 25 mL flask attached to a gas buret and immersed in a 30°C bath (eq S1 and Figure S2 in the Supporting Information), and the mixture was vigorously shaken (500 rpm) during the run. The reaction was monitored by measuring the volume of the evolved hydrogen with time until hydrogen evolution stopped. Representative gas vs time plots are given in the Supporting Information. The solution was then passed through a silica gel column. Removal of the volatiles gave the boryl ether. The products were analyzed by ^1H , $^{13}\text{C}\{^1\text{H}\}$, and ^{11}B NMR spectroscopy.

Spectroscopic Data of the Products of the Alcoholysis. **MeOBpin.** ^1H NMR (400 MHz, C_6D_6 , 293 K): δ 1.04 (s, 12 H, $\text{CH}_3\text{-BPin}$), 3.50 (s, 3 H, $-\text{OCH}_3$). $^{13}\text{C}\{^1\text{H}\}$ -APT NMR (100.6 MHz, C_6D_6 , 293 K): δ 82.6 (s, C-Bpin), 52.4 (s, $-\text{OCH}_3$), 24.8 (s, $\text{CH}_3\text{-BPin}$). ^{11}B NMR (96.3 MHz, C_6D_6 , 293 K): 22.9 (s).

EtOBpin. ^1H NMR (400 MHz, C_6D_6 , 293 K): δ 3.87 (q, $J_{\text{H-H}} = 7.2$, 2 H, $-\text{OCH}_2\text{CH}_3$), 1.08 (t, $J_{\text{H-H}} = 7.2$, 3 H, $-\text{OCH}_2\text{CH}_3$), 1.05 (s, 12 H, $\text{CH}_3\text{-BPin}$). $^{13}\text{C}\{^1\text{H}\}$ -APT NMR (100.6 MHz, C_6D_6 , 293 K): δ 82.4 (s, C-Bpin), 60.7 (s, $-\text{OCH}_2\text{CH}_3$), 24.8 (s, $\text{CH}_3\text{-BPin}$), 17.5 (s, $-\text{OCH}_2\text{CH}_3$). ^{11}B NMR (96.3 MHz, C_6D_6 , 293 K): 22.6 (s).

$n\text{BuOBPin}$. ^1H NMR (400 MHz, C_6D_6 , 293 K): δ 3.83 (t, $J_{\text{H-H}} = 6.4$, 2 H, $-\text{OCH}_2(\text{CH}_2)_2\text{CH}_3$), 1.46 and 1.27 (both m, 2 H each, $-\text{OCH}_2(\text{CH}_2)_2\text{CH}_3$), 1.06 (s, 12 H, $\text{CH}_3\text{-BPin}$), 0.79 (t, $J_{\text{H-H}} = 7.6$, 3 H, $-\text{OCH}_2(\text{CH}_2)_2\text{CH}_3$). $^{13}\text{C}\{^1\text{H}\}$ -APT NMR (100.6 MHz, C_6D_6 , 293 K): δ 82.4 (s, C-Bpin), 64.7 (s, $-\text{OCH}_2(\text{CH}_2)_2\text{CH}_3$), 34.1 and 19.2 (both s, $-\text{OCH}_2(\text{CH}_2)_2\text{CH}_3$), 24.8 (s, $\text{CH}_3\text{-BPin}$), 13.9 (s, $-\text{OCH}_2(\text{CH}_2)_2\text{CH}_3$). ^{11}B NMR (96.3 MHz, C_6D_6 , 293 K): 22.6 (s).

$n\text{OctyOBPin}$. ^1H NMR (400 MHz, C_6D_6 , 293 K): δ 3.84 (t, $J_{\text{H-H}} = 6.4$, 2 H, $-\text{OCH}_2(\text{CH}_2)_7\text{CH}_3$), 1.50 (m, 2 H, $-\text{OCH}_2(\text{CH}_2)_7\text{CH}_3$),

1.3–1.2 (m, 10 H, CH₂), 1.07 (s, 12 H, CH₃-BPin), 0.84 (t, $J_{\text{H-H}} = 7.2$, 3 H, $-\text{OCH}_2(\text{CH}_2)_7\text{CH}_3$). ¹³C{¹H}-APT NMR (100.6 MHz, C₆D₆, 293 K): δ 82.4 (s, C-Bpin), 65.1 (s, $-\text{OCH}_2(\text{CH}_2)_7\text{CH}_3$), 32.3, 32.1, 29.7, 26.1, and 23.1 (all s, $-\text{OCH}_2(\text{CH}_2)_7\text{CH}_3$), 24.8 (s, CH₃-BPin), 14.4 (s, $-\text{OCH}_2(\text{CH}_2)_7\text{CH}_3$). ¹¹B NMR (96.3 MHz, C₆D₆, 293 K): 22.5 (s).

PhCH₂OBPIn. ¹H NMR (400 MHz, C₆D₆, 293 K): δ 7.3–7.0 (m, 5 H, CH-Ph), 4.87 (s, 2 H, $-\text{OCH}_2\text{Ph}$), 0.99 (s, 12 H, CH₃-BPin). ¹³C{¹H}-APT NMR (100.6 MHz, C₆D₆, 293 K): δ 140.0 (s, C_{ipso}-Ph), 128.6, 127.6, and 127.0 (all s, CH-Ph), 82.8 (s, C-Bpin), 66.9 (s, $-\text{OCH}_2\text{Ph}$), 24.7 (s, CH₃-BPin). ¹¹B NMR (96.3 MHz, C₆D₆, 293 K): 22.9 (s).

ⁱPrOBPin. ¹H NMR (400 MHz, C₆D₆, 293 K): δ 4.39 (m, 1 H, CH-ⁱPr), 1.13 (d, $J_{\text{H-H}} = 6.0$, 6 H, CH₃-ⁱPr), 1.06 (s, 12 H, CH₃-BPin). ¹³C{¹H}-APT NMR (100.6 MHz, C₆D₆, 293 K): δ 82.2 (s, C-Bpin), 67.3 (s, CH-ⁱPr), 24.8 (s, CH₃-BPin), 24.6 (s, CH₃-ⁱPr). ¹¹B NMR (96.3 MHz, C₆D₆, 293 K): 22.3 (s).

^tBuOBPin. ¹H NMR (400 MHz, C₆D₆, 293 K): δ 1.32 (s, 9 H, CH₃-^tBu), 1.05 (s, 12 H, CH₃-BPin). ¹³C{¹H}-APT NMR (100.6 MHz, C₆D₆, 293 K): δ 81.8 (s, C-Bpin), 73.5 (s, C-^tBu), 30.3 (s, CH₃-^tBu), 24.7 (s, CH₃-BPin). ¹¹B NMR (96.3 MHz, C₆D₆, 293 K): 21.7 (s).

PhOBPin. ¹H NMR (400 MHz, C₆D₆, 293 K): δ 7.2–6.8 (m, 5 H, CH-Ph), 1.00 (s, 12 H, CH₃-BPin). ¹³C{¹H}-APT NMR (100.6 MHz, C₆D₆, 293 K): δ 154.3 (s, C_{ipso}-Ph), 129.6, 123.3, and 120.0 (all s, CH-Ph), 83.4 (s, C-Bpin), 24.6 (s, CH₃-BPin). ¹¹B NMR (96.3 MHz, C₆D₆, 293 K): 22.2 (s).

Hydrolysis Reactions of Pinacolborane Catalyzed by OsCl₂(κ^2 -C,C-[CN(CH₃)CHCHNCH₂C(O)])(P^{*i*}Pr)₂ (3). The hydrolysis reactions were carried out by the same procedure as the alcoholysis but using water instead of alcohols (eq S2 in the Supporting Information). Since the product obtained is an alcohol (HOBPin), a second addition of HBPIn was injected in order to obtain (Bpin)₂O.

Spectroscopic Data of the Products of the Hydrolysis. **HOBPin.** ¹H NMR (400 MHz, C₆D₆, 293 K): δ 6.56 (br, 1 H, $-\text{OH}$), 1.02 (s, 12 H, CH₃-BPin). ¹³C{¹H}-APT NMR (100.6 MHz, C₆D₆, 293 K): δ 83.0 (s, C-Bpin), 24.6 (s, CH₃-BPin). ¹¹B NMR (96.3 MHz, C₆D₆, 293 K): 21.8 (s).

(Bpin)₂O. ¹H NMR (300 MHz, C₆D₆, 293 K): δ 1.01 (s, 24 H, CH₃-BPin). ¹³C{¹H}-APT NMR (75.5 MHz, C₆D₆, 293 K): δ 83.0 (s, C-BPin), 24.7 (s, CH₃-BPin). ¹¹B NMR (96.3 MHz, C₆D₆, 293 K): 21.7 (s).

Structural Analysis of Complexes 3–6. X-ray data were collected for the complexes on a Bruker Smart APEX CCD diffractometer equipped with a normal focus, 2.4 kW sealed tube source (Mo radiation, $\lambda = 0.71073$ Å) operating at 50 kV and 40 mA (5) or 30 mA (3, 4, and 6). Data were collected over the complete sphere. Each frame exposure time was 10 s (3, 4, and 6) or 40 s (5) covering 0.3° in ω . Data were corrected for absorption by using a multiscan method applied with the SADABS program.²⁵ The structures were solved by Patterson or direct methods and refined by full-matrix least squares on F^2 with SHELXL97,²⁶ including isotropic and subsequently anisotropic displacement parameters. The hydrogen atoms (except hydrides) were observed in the least-squares Fourier maps or calculated and refined freely or refined using a restricted riding model. Hydrogens bonded to metal atoms were observed in the last cycles of refinement but refined too close to metals; therefore, a restricted refinement model was used for all of them ($d(\text{Os}–\text{H}) = 1.59(1)$ Å).

Complex 6 was first solved and refined in the monoclinic *Cc* space group. However, a pseudomerohedric twin that simulated orthorhombic (β approximately 90°) and racemic twin laws was observed. Once the refinement was finished, the ADDSYM option in Platon²⁷ suggested the orthorhombic *Cmcm* as the correct space group.²⁸ With this symmetry, the osmium is site in the 2-fold axis along (1/2, y , 3/4). As a result, the chlorine, carbene, and dihydrogen ligands are disordered by symmetry. To complete the anisotropic refinement, restraints were used in some distances (DFIX command) and thermal parameters (SIMU and DELU commands) in the disordered groups.

Crystal data for 3: C₂₄H₄₉ClN₂OOSp₂·2C₃H₆O, M_w 785.40, orange, irregular block (0.21 × 0.10 × 0.08 mm), orthorhombic, space group *Pnma*, $a = 17.4627(7)$ Å, $b = 22.0671(9)$ Å, $c = 9.0470(4)$ Å, $V = 3486.3(3)$ Å³, $Z = 4$, $Z' = 0.5$, $D_{\text{calc}} = 1.496$ g cm^{−3}, $F(000) = 1608$, $T = 100(2)$ K, $\mu = 3.857$ mm^{−1}, 40171 measured reflections ($2\theta = 3–58^\circ$, ω scans 0.3°), 4389 unique reflections ($R_{\text{int}} = 0.0376$), minimum/maximum transmission factors 0.630/0.862, final agreement factors $R1 = 0.0215$ (3924 observed reflections, $I > 2\sigma(I)$) and $wR2 = 0.0482$, data/restraints/parameters 4389/0/202; GOF = 1.040, largest peak and hole 0.972 (close to osmium atom) and -0.688 e/Å³.

Crystal data for 4: C₂₅H₄₉ClN₂O₂OsP₂·2C₃H₆O, M_w 813.41, colorless, irregular block (0.13 × 0.06 × 0.06 mm), orthorhombic, space group *Pbcm*, $a = 9.0903(4)$ Å, $b = 18.0138(8)$ Å, $c = 22.3303(10)$ Å, $V = 3656.6(3)$ Å³, $Z = 4$, $Z' = 0.5$, $D_{\text{calc}} = 1.478$ g cm^{−3}, $F(000) = 1664$, $T = 100(2)$ K, $\mu = 3.682$ mm^{−1}, 30916 measured reflections ($2\theta = 3–58^\circ$, ω scans 0.3°), 4527 unique ($R_{\text{int}} = 0.0436$), minimum/maximum transmission factors 0.630/0.862, final agreement factors $R1 = 0.0269$ (4011 observed reflections, $I > 2\sigma(I)$) and $wR2 = 0.0548$, data/restraints/parameters 4527/0/214, GOF = 1.079, largest peak and hole 1.281 (close to osmium atoms) and -1.630 e/Å³.

Crystal data for 5: C₂₄H₄₉ClN₂O₃OsP₂, M_w 701.24, red, irregular block (0.25 × 0.06 × 0.02 mm), orthorhombic, space group *Pbca*, $a = 16.723(6)$ Å, $b = 16.459(6)$ Å, $c = 21.160(7)$ Å, $V = 5824(3)$ Å³, $Z = 8$, $Z' = 1$, $D_{\text{calc}} = 1.599$ g cm^{−3}, $F(000) = 2832$, $T = 150(2)$ K, $\mu = 4.607$ mm^{−1}, 26726 measured reflections ($2\theta = 3–51^\circ$, ω scans 0.3°), 5341 unique ($R_{\text{int}} = 0.1805$), minimum/maximum transmission factors 0.510/0.862, final agreement factors $R1 = 0.0564$ (2838 observed reflections, $I > 2\sigma(I)$) and $wR2 = 0.1157$, data/restraints/parameters 5341/6/311, GOF = 0.974, largest peak and hole 1.556 (close to osmium atoms) and -1.925 e/Å³.

Crystal data for 6: C₂₄H₅₁ClN₂O₁OsP₂·2C₃H₆O, M_w 787.41, orange, irregular block (0.15 × 0.12 × 0.11 mm), orthorhombic, space group *Cmcm*, $a = 11.2351(6)$ Å, $b = 14.6065(8)$ Å, $c = 21.7840(12)$ Å, $V = 3574.9(3)$ Å³, $Z = 4$, $Z' = 0.5$, $D_{\text{calc}} = 1.463$ g cm^{−3}, $F(000) = 1616$, $T = 100(2)$ K, $\mu = 3.762$ mm^{−1}, 29295 measured reflections ($2\theta = 3–58^\circ$, ω scans 0.3°), 2388 unique ($R_{\text{int}} = 0.0376$), minimum/maximum transmission factors 0.641/0.746, final agreement factors $R1 = 0.0228$ (2335 observed reflections, $I > 2\sigma(I)$) and $wR2 = 0.0556$, data/restraints/parameters 2388/109/143, GOF = 1.086, largest peak and hole 1.808 and -1.464 e/Å³.

■ ASSOCIATED CONTENT

Supporting Information

Figures and CIF files giving positional displacement parameters, crystallographic data, and bond lengths and angles of compounds 3–6, IR spectrum of complex 5, NMR spectra of complexes 5, 6, 6', and 7, and plots of hydrogen evolution versus time for the alcoholysis and hydrolysis of pinacolborane catalyzed by complex 3. The Supporting Information is available free of charge on the ACS Publications website at DOI: 10.1021/acs.organomet.5b00418.

■ AUTHOR INFORMATION

Corresponding Authors

*E-mail for M.A.E.: maester@unizar.es.

*E-mail for M.Y.: yus@ua.es.

Notes

The authors declare no competing financial interest.

■ ACKNOWLEDGMENTS

Financial support from the MINECO of Spain (Projects CTQ2014-52799-P and CTQ2014-51912-RED), the Diputación General de Aragón (E-35), and the European Social Fund (FSE) and FEDER. M.P.G. thanks the Spanish MINECO for her FPI fellowship. T.B. thanks the Spanish MINECO for funding through the Juan de la Cierva program.

REFERENCES

- (1) (a) Askevold, B.; Roesky, H. W.; Schneider, S. *ChemCatChem* **2012**, *4*, 307–320. (b) Waterman, R. *Chem. Soc. Rev.* **2013**, *42*, 5629–5641.
- (2) Grützmacher, H. *Angew. Chem., Int. Ed.* **2008**, *47*, 1814–1818.
- (3) (a) Noyori, R.; Ohkuma, T. *Angew. Chem., Int. Ed.* **2001**, *40*, 40–73. (b) Clapham, S. E.; Hadzovic, A.; Morris, R. H. *Coord. Chem. Rev.* **2004**, *248*, 2201–2237.
- (4) Conley, B. L.; Pennigton-Boggio, M. K.; Boz, E.; Williams, T. J. *Chem. Rev.* **2010**, *110*, 2294–2312.
- (5) Gunanathan, C.; Milstein, D. *Acc. Chem. Res.* **2011**, *44*, 588–602.
- (6) Nelson, D. J.; Nolan, S. P. *Chem. Soc. Rev.* **2013**, *42*, 6723–6753.
- (7) (a) Kantchev, E. A. B.; O'Brien, C. J.; Organ, M. G. *Angew. Chem., Int. Ed.* **2007**, *46*, 2768–2813. (b) Díez-González, S.; Marion, N.; Nolan, S. P. *Chem. Rev.* **2009**, *109*, 3612–3676.
- (8) Kühn, O. *Chem. Soc. Rev.* **2007**, *36*, 592–607. (b) John, A.; Ghosh, P. *Dalton Trans.* **2010**, *39*, 7183–7206.
- (9) For some representative examples, see: (a) McGuinness, D. S.; Cavell, K. J. *Organometallics* **2000**, *19*, 741–748. (b) Peñafiel, I.; Pastor, I. M.; Yus, M.; Esteruelas, M. A.; Oliván, M.; Oñate, E. *Eur. J. Org. Chem.* **2011**, 7174–7181. (c) Bartoszewicz, A.; Marcos, R.; Sahoo, S.; Inge, A. K.; Zou, X.; Martin-Matute, B. *Chem. - Eur. J.* **2012**, *18*, 14510–14519. (d) Peñafiel, I.; Pastor, I. M.; Yus, M.; Esteruelas, M. A.; Oliván, M. *Organometallics* **2012**, *31*, 6154–6161.
- (10) (a) Miranda-Soto, V.; Grotjahn, D. B.; Cooksy, A. L.; Golen, J. A. *Angew. Chem., Int. Ed.* **2011**, *50*, 631–635. (b) Kösterke, T.; Pape, T.; Hahn, F. E. J. *J. Am. Chem. Soc.* **2011**, *133*, 2112–2115. (c) Brackemeyer, D.; Hervé, A.; Schulte to Brinke, C.; Jahnke, M. C.; Hahn, F. E. J. *Am. Chem. Soc.* **2014**, *136*, 7841–7844. (d) Das, R.; Daniliuc, C. G.; Hahn, F. E. *Angew. Chem., Int. Ed.* **2014**, *53*, 1163–1166.
- (11) (a) Baya, M.; Eguillor, B.; Esteruelas, M. A.; Oliván, M.; Oñate, E. *Organometallics* **2007**, *26*, 6556–6563. (b) Eguillor, B.; Esteruelas, M. A.; Oliván, M.; Puerta, M. *Organometallics* **2008**, *27*, 445–450. (c) Alabau, R. G.; Eguillor, B.; Esler, J.; Esteruelas, M. A.; Oliván, M.; Oñate, E.; Tsai, J.-Y.; Xia, C. *Organometallics* **2014**, *33*, 5582–5596. (d) Bolaño, T.; Esteruelas, M. A.; Fernández, I.; Oñate, E.; Palacios, A.; Tsai, J.-Y.; Xia, C. *Organometallics* **2015**, *34*, 778–789.
- (12) See for example: (a) Barrio, P.; Castarlenas, R.; Esteruelas, M. A.; Oñate, E. *Organometallics* **2001**, *20*, 2635–2638. (b) Esteruelas, M. A.; Masamunt, A. B.; Oliván, M.; Oñate, E.; Valencia, M. J. *Am. Chem. Soc.* **2008**, *130*, 11612–11613. (c) Crespo, O.; Eguillor, B.; Esteruelas, M. A.; Fernández, I.; García-Raboso, J.; Gómez-Gallego, M.; Martín-Ortiz, M.; Oliván, M.; Sierra, M. A. *Chem. Commun.* **2012**, *48*, 5328–5330.
- (13) Eguillor, B.; Esteruelas, M. A.; García-Raboso, J.; Oliván, M.; Oñate, E.; Pastor, I.; Peñafiel, I.; Yus, M. *Organometallics* **2011**, *30*, 1658–1667.
- (14) Fei, Z.; Zhao, D.; Geldbach, T. J.; Scopelliti, R.; Dyson, P. J. *Chem. - Eur. J.* **2004**, *10*, 4886–4893.
- (15) See for example: (a) Barrio, P.; Esteruelas, M. A.; Oñate, E. *Organometallics* **2004**, *23*, 1340–1348. (b) Esteruelas, M. A.; Hernández, Y. A.; López, A. M.; Oliván, M.; Rubio, L. *Organometallics* **2008**, *27*, 799–802.
- (16) (a) Aubert, M.; Bellachioma, G.; Cardaci, G.; Macchioni, A.; Reinchenbach, G.; Burla, M. C. *J. Chem. Soc., Dalton Trans.* **1997**, 1759–1764. (b) Watson, W. H.; Huang, S.-H.; Richmond, M. G. J. *J. Chem. Crystallogr.* **2007**, *37*, 479–482. (c) Bajo, S.; Esteruelas, M. A.; López, A. M.; Oñate, E. *Organometallics* **2014**, *33*, 4057–4066.
- (17) (a) Maddock, S. M.; Richard, C. E. F.; Roper, W. R.; Wright, L. J. *J. Organomet. Chem.* **1996**, *510*, 267–279. (b) Bartucz, T. Y.; Galombek, A.; Lough, A. J.; Maltby, P. A.; Morris, R. H.; Ramachandran, R.; Schlaf, M. *Inorg. Chem.* **1998**, *37*, 1555–1562. (c) Barthazy, P.; Wörle, M.; Rüegger, H.; Mezzetti, A. *Inorg. Chem.* **2000**, *39*, 4903–4912.
- (18) For some relevant compounds of these types of metals of the platinum group, see for example: (a) Jia, G.; Ng, W. S.; Chu, H. S.; Wong, W.-T.; Yu, N.-T.; Williams, I. D. *Organometallics* **1999**, *18*, 3597–3602. (b) Hüller, L. J. L.; Mas-Marzá, E.; Moreno, A.; Lowe, J. P.; McGregor, S. A.; Mahon, M. F.; Pregosin, P. S.; Whittlesey, M. K. *J. Am. Chem. Soc.* **2009**, *131*, 9618–9619. (c) Zenkina, O. V.; Keske, E. C.; Wang, R.; Crudden, C. M. *Angew. Chem., Int. Ed.* **2011**, *50*, 8100–8104. (d) Boisvert, L.; Goldberg, K. I. *Acc. Chem. Res.* **2012**, *45*, 899–910.
- (19) (a) Moers, F. G.; Hoedt, R. W. M.; Langhout, J. P. *J. Inorg. Nucl. Chem.* **1974**, *36*, 2279–2282. (b) Parent, J. S.; McManus, N. T.; Rempel, G. L.; Poer, W. P.; Marder, T. B. *J. Mol. Catal. A: Chem.* **1998**, *135*, 285–293.
- (20) (a) Esteruelas, M. A.; Sola, E.; Oro, L. A.; Meyer, U.; Werner, H. *Angew. Chem., Int. Ed. Engl.* **1988**, *27*, 1563–1564. (b) Esteruelas, M. A.; García-Obregón, T.; Herrero, J.; Oliván, M. *Organometallics* **2011**, *30*, 6402–6407.
- (21) Bautista, M. T.; Cappellari, E. P.; Drouin, S. D.; Morris, R. H.; Schweitzer, C. T.; Sella, A.; Zubkowski, J. *J. Am. Chem. Soc.* **1991**, *113*, 4876–4887.
- (22) (a) Maltby, P. A.; Schlaf, M.; Steinbeck, M.; Lough, A. J.; Morris, R. H.; Klooster, W. T.; Koetzle, T. F.; Srivastara, R. C. *J. Am. Chem. Soc.* **1996**, *118*, 5396–5407. (b) Luther, T. A.; Heinekey, D. M. *Inorg. Chem.* **1998**, *37*, 127–132.
- (23) Esteruelas, M. A.; López, A. M.; Mora, M.; Oñate, E. *Chem. Commun.* **2013**, *49*, 7543–7545.
- (24) Aracama, M.; Esteruelas, M. A.; Lahoz, F. J.; López, J. A.; Meyer, U.; Oro, L. A.; Werner, H. *Inorg. Chem.* **1991**, *30*, 288–293.
- (25) Blessing, R. H. *Acta Crystallogr., Sect. A: Found. Crystallogr.* **1995**, *51*, 33. SADABS: Area-detector absorption correction; Bruker-AXS, Madison, WI, 1996.
- (26) SHELXTL Package v. 6.14; Bruker-AXS, Madison, WI, 2000. Sheldrick, G. M. *Acta Crystallogr., Sect. A: Found. Crystallogr.* **2008**, *64*, 112–122.
- (27) Spek, A. L. *J. Appl. Crystallogr.* **2003**, *36*, 7.
- (28) See for example: Zakaria, C. M.; Ferguson, G.; Lough, A.; Glidewell, C. *Acta Crystallogr., Sect. C: Cryst. Struct. Commun.* **2003**, *59*, m271.